Bis(η-*tert*-butylcyclopentadienyl)hydridoniobium Ditelluride, a Convenient Reagent for the Synthesis of Polynuclear Metal Telluride Complexes

Henri Brunner,[a] Helene Cattey,[b] David Evrard,[b] Marek M. Kubicki,[b] Yves Mugnier,[b] Estelle Vigier,[b] Joachim Wachter,*[a] Robert Wanninger,[a] and Manfred Zabel[a]

Keywords: Niobium / Tellurium / Polynuclear complexes / Cyclopentadienyl complexes / Electrochemistry

Reaction of $[Cp'_2NbH_3]$ ($Cp' = tBuC_5H_4$) with Te powder in THF gives $[Cp'_2Nb(Te_2)H]$ (**1**) and $[Cp'_6Nb_4Te_4O]$ (**2**). The yield of **1** varies between 10 and 81% depending on the degree of oxygen contamination of the reagents. Complexes **1** and **2** react with $[Cr(CO)_5THF]$ to give $[Cp'_2Nb(Te_2)H{\cdot}Cr(CO)_5]$ (**3**) and $[Cp'_6Nb_4Te_4O{\cdot}2Cr(CO)_5]$ (**4**), respectively. The crystal structures of **2**–**4** have been determined. In **3** a Te_2 unit and an H ligand are coordinated to a bent niobocene moiety; the $Cr(CO)_5$ group is attached to the lateral Te atom. The molecular cores of **2** and **4** are practically identical in that they contain two planar Nb_2Te_2 rings connected by a nearly linear oxygen bridge. Each of the "outer" Nb atoms bears two Cp′ ligands, whereas the "inner" Nb atom only has one such ligand. An additional structural feature in **4** is two $Cr(CO)_5$ groups, attached to one Te bridge of each Nb_2Te_2 ring. Thermolysis of **3** leads to the formation of diamagnetic $[Cp'_4Nb_2Te_2]$ (**5**), which also contains a planar Nb_2Te_2 core. The relatively long transannular Nb–Nb distance (3.647 Å) is consistent, according to DFT calculations, with a through-space Nb–Nb coupling. Complex **5** reacts with CH_3I with successive methylation of both Te bridges to give $[Cp'_4Nb_2Te(CH_3Te)]I$ (**[6]I**) and $[Cp'_4Nb_2(CH_3Te)_2]I_2$ (**[7]I_2**). The crystal structure of **[7]I_2** may be derived from that of **5**, the incoming CH_3 groups being fixed at the Te bridges in a *trans* position. ^1H NMR spectroscopic investigations reveal a restricted rotation around the Cp′–Nb bonds in **2** and **5** at –90 °C and in **4** and **[7]I_2** at ambient temperature. Electrochemical studies have been carried out on **5**, **[6]I**, and **[7]I_2**, showing that all compounds undergo two reversible one-electron reduction steps. The reduction potential decreases by ca. 1.6 V when going from **5** to **[7]I_2**. There is also a clear linear correlation between the reduction potentials measured for **5** to **[7]I_2** and the energies of the corresponding LUMO's calculated at the DFT/B3LYP level. These LUMO's bear some 70% contribution from both Nb atoms and, consequently, the reduction processes mainly operate at both metallic centers.

Introduction

Group 4 and 5 metallocene derivatives of the heavier chalcogens Se and Te are an attractive target for reactivity studies.[1−3] Recent examples include ligand rearrangements[4−6] and the stabilization of labile seleno- and telluroorganic ligands.[3,4] Niobocene or tantalocene dichalcogenides exist in the isomeric forms **A**−**C**, and depending on the nature of the cyclopentadienyl ligand (Cp) and the chalcogen X (X = Se or Te) the additional hydrogen is found in different bonding modes.[6] The only known example of isomer **A** is $[Cp^*_2Nb(\eta^2\text{-}Te_2H)]$ in which the Nb center bears electron-rich peralkylated C_5Me_5 (Cp^*) ligands along with a hydrogenditelluride ligand.[7] Its reactivity is characterized by an easy loss of Te^0 [7] or Te^{2-} [8−11] in the presence of reactive transition metal fragments, which finally leads to a series of homo- and heterometallic telluride clusters.

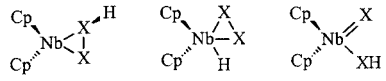

A **B** **C**

It has already been established that the formation of related niobocene sulfides strongly depends on the substituents at the Cp ligand.[12] Therefore, we decided to investigate the reaction of $[Cp'_2NbH_3]$ ($Cp' = tBuC_5H_4$) with tellurium. Our investigations show that the replacement of the electron-rich C_5Me_5 ligand by Cp′ exerts considerable influence on the electronic and steric parameters as well as on the subsequent formation of polynuclear metal telluride complexes.

Results and Discussion

Preparation and Characterization of Complexes 1−4

Reaction of $[Cp'_2NbH_3]$ with 2.5 equivalents of carefully degassed tellurium powder in freshly distilled THF at 40 °C

[a] Institut für Anorganische Chemie, Universität Regensburg, 93040 Regensburg, Germany
[b] Laboratoire de Synthèse et d'Electrosynthèse Organométalliques (UMR 5632), Université de Bourgogne, 21100 Dijon, France

gave dark orange $[Cp'_2Nb(Te_2)H]$ (**1**) in 81% yield. However, in the presence of traces of air complex **1** was obtained in yields of between 10 and 32% and red-violet $[Cp'_6Nb_4Te_4O]$ (**2**) formed in yields from 9−53% as an additional product (Scheme 1). Similar results were obtained in toluene at 80 °C. Solutions of **1** are very sensitive towards air and even the solid decomposes slowly when stored at −20 °C. In boiling toluene **1** slowly converts into **2**. In a typical example 18% of **2** was formed after 24 h. This behavior is in contrast with that of the structurally related $[Cp^*_2Ta(Te_2)H]$, which transforms into $[Cp^*_2Ta(=Te)H]$ under similar conditions.[4]

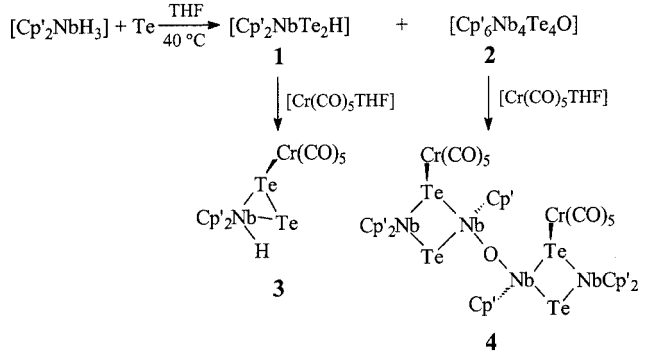

Scheme 1

The composition of complexes **1** and **2** was determined from FD mass spectra and confirmed by elemental analyses. The latter, however, gives good results only for **2** as the values obtained for **1** are always a little bit too low. Correct analytical data have been obtained for the $Cr(CO)_5$ adduct **3** (see below), which has successfully been subjected to an X-ray crystallographic investigation.

The ^1H NMR spectrum of **1** at room temperature as well as at −90 °C shows four multiplets of equal intensities for the aromatic protons and one singlet at $\delta = 1.39$ for the *t*Bu groups. An additional signal at $\delta = -3.50$ is observed with $^2J(H\text{-}^{125}Te) = 86.7$ Hz. One Te resonance was found by means of $^1H\text{-}^{125}Te$ polarization transfer techniques and this was confirmed in the ^{125}Te NMR spectrum, which revealed only one broad resonance ($h_{1/2} \approx 300$ Hz) at $\delta = -749.4$. The second resonance cannot be detected, probably due to partially relaxed scalar $^{125}Te\text{-}^{93}Nb$ interactions. Unfortunately, similar problems prevented the observation of ^{125}Te NMR spectra for the other compounds. An X-ray diffraction analysis carried out on $[Cp'_2Nb(Te_2)H{\cdot}Cr(CO)_5]$ (**3**) (see below) provides evidence for the presence of a $\mu,\eta^{1:2}\text{-}Te_2$ ligand. Localization of a hydride directly bonded to the Nb center and lying in the $NbTe_2$ plane allows for the determination of **3**, and very likely **1**, from the structural form **B**. Structural analogs of **1** are $[Cp^*_2Ta(Te_2)H]$,[4] $[Cp'_2Ta(S_2)H]$,[13] and $[Cp^*_2Nb(S_2)H]$.[12a] There is no evidence for the existence of any other isomeric form.

An X-ray diffraction analysis of a single crystal of **2** shows two planar Nb_2Te_2 rings (Figure 1) connected by an oxygen bridge. Each of the "outer" Nb atoms [Nb(1), Nb(4)] bears two Cp′ ligands, whereas the coordination sphere of the "inner" Nb atoms [Nb(2), Nb(3)] is completed by only one Cp′ ligand, thus forming two $Cp'_3Nb_2Te_2$ units. The linearity of the Nb−O−Nb bridge [angle (Nb−O−Nb) = 177.1(1)°] evokes a contribution of p_π oxygen orbitals as has been suggested for other linearly O-bridged bimetallic complexes.[14] The fact that the observed Nb−O distances [mean 1.909(2) Å] are longer than Nb=O bonds in oxoniobocene complexes (1.63−1.741 Å)[15] is not in contradiction with the above argument.[14] Within the Nb_2Te_2 rings there are two different Nb−Te distances. The Nb−Te bonds around Nb(2) and Nb(3) are shorter than the bonds around Nb(1) and Nb(4), by 0.18 Å (Table 1). They are also slightly shorter than typical Nb−Te single bonds.[16] Striking differences are found for the Te−Nb−Te angles, they range from 96.4(1)° [Te(3)−Nb(4)−Te(4)] to 107.1(1)° [Te(1)−Nb(2)−Te(2)], thus reflecting the different coordination spheres around both niobium centers. A similar structure has been found in $[Cp'_6V_4S_4O]$.[17]

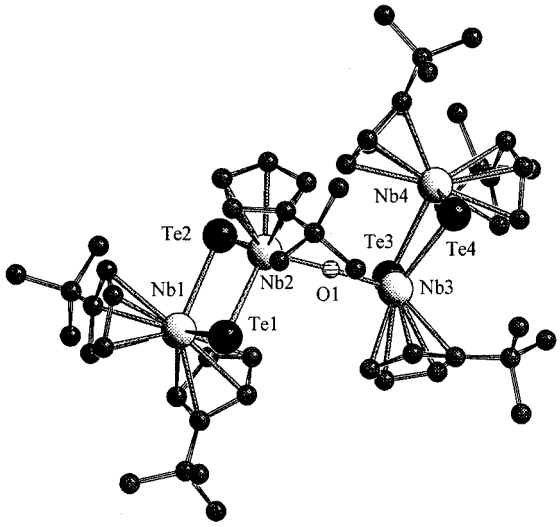

Figure 1. Molecular structure of $[Cp'_6Nb_4Te_4O]$ (**2**) (Schakal)

The diamagnetic nature of the molecule is deduced from its ^1H NMR spectrum (see below) and it may be explained by the presence of direct Nb−Nb interactions: Whereas the Te−Te distances (4.236 Å) approximately correspond to the sum of the van der Waals radii[18] the Nb−Nb distances (3.43 Å) are only slightly longer than those in $[(C_5H_5)_2Nb(\mu\text{-}S)]_2$ [*d*(Nb−Nb) 3.2340(8) Å][19] or in $[C_5H_5(C_5H_4)NbH]_2$ (3.105 Å),[20] for which Nb−Nb bonds have been postulated. The possibility of through-space Nb−Nb coupling in complexes containing Nb_2Te_2 rings has been investigated for compounds **5**, **[6]I**, and **[7]I_2** (see below).

The crystal structure of **2** also reveals that the bulky *t*Bu groups in the niobocene units "Nb(1)" and "Nb(4)" are oriented in a staggered conformation. The concerned $t\text{Bu}-Cp_{center}/t\text{Bu}-Cp'_{center}$ torsional angles are about 122°. Recently it has been shown that for bent group 4 metallocenes like $[(t\text{Bu}C_5H_4)_2ZrX_2]$ (X = halogen, alkyl, aryl), chiral ground-state geometries are able to epimerize upon rotation around the Cp′−metal bond.[21] The activation barrier for this rotation depends on the interaction of

Table 1. Selected distances [Å] and angles [°] for $[Cp'_6Nb_4Te_4O]$ (**2**) and $[Cp'_6Nb_4Te_4O{\cdot}2Cr(CO)_5]$ (**4**)

	2	**4**
Nb(1)−Te(1)	2.829(1)	2.809(1)
Nb(1)−Te(2)	2.809(1)	2.836(1)
Nb(2)−Te(1)	2.648(1)	2.632(1)
Nb(2)−Te(2)	2.641(1)	2.678(1)
Nb(2)−O(1)	1.914(2)	1.896(4)
Nb(3)−O(1)	1.904(2)	1.923(4)
Nb(3)−Te(3)	2.644(1)	2.633(1)
Nb(3)−Te(4)	2.642(1)	2.660(1)
Nb(4)−Te(3)	2.832(1)	2.821(1)
Nb(4)−Te(4)	2.829(1)	2.827(1)
Te(2)−Cr(1)		2.760(1)
Te(4)−Cr(2)		2.737(1)
Te(1)−Nb(1)−Te(2)	97.9(1)	98.7(1)
Te(1)−Nb(2)−Te(2)	107.1(1)	107.4(1)
Te(3)−Nb(3)−Te(4)	105.9(1)	105.9(1)
Te(3)−Nb(4)−Te(4)	96.4(1)	96.8(1)
Te(1)−Nb(2)−O(1)	106.4(1)	104.5(1)
Te(2)−Nb(2)−O(1)	100.7(1)	99.6(1)
Te(3)−Nb(3)−O(1)	104.0(1)	102.4(1)
Te(4)−Nb(3)−O(1)	102.4(1)	99.4(1)
Nb(2)−O(1)−Nb(3)	177.2(1)	175.9(2)
Cr(1)−Te(2)−Nb(2)		131.6(1)
Cr(1)−Te(2)−Nb(1)		128.8(1)
Cr(2)−Te(4)−Nb(3)		132.8(1)
Cr(2)−Te(4)−Nb(4)		130.3(1)
$C(1-5)_{center}$−Nb(1)−$C(10-14)_{center}$	134.2(1)	134.0(1)
$C(37-41)_{center}$−Nb(4)−$C(46-50)_{center}$	133.0(1)	133.1(1)

the Cp′-bonded substituent with the ligands X. In our case the ^{1}H NMR spectrum of **2** shows five signals of intensity 4:4:4:8:4 between δ = 4.18 and 5.75 for the C_5H_4 protons, at room temperature. Three singlets of equal intensities are observed for the six *t*Bu groups. Upon cooling to −90 °C the diastereotopic cyclopentadienyl protons split into several broad multiplets, while the *t*Bu groups give a set of not very well resolved signals (Figure 2). A much better resolution into distinct resonances is achieved in the sterically crowded $Cr(CO)_5$ adduct **4** (see below, Figure 2) even at room temperature.

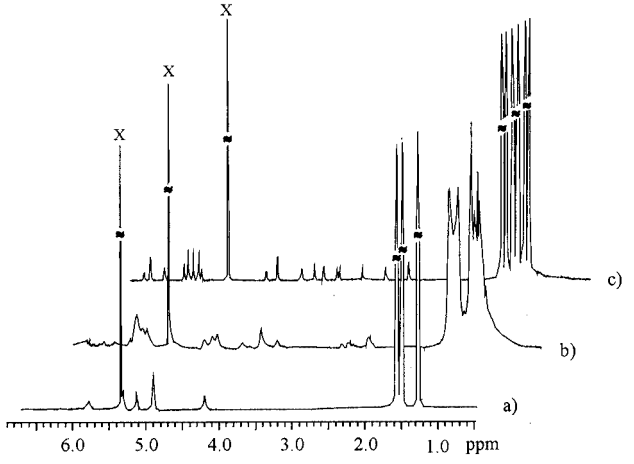

Figure 2. ^{1}H NMR spectra (*t*BuC_5H_4 signals) of **2** at 24 °C (a) and −90 °C (b), and of **4** at 24 °C (c) (X: CH_2Cl_2)

Reaction of $[Cp'_2NbTe_2H]$ with an excess of $[Cr(CO)_5THF]$ gave $[Cp'_2NbTe_2H{\cdot}Cr(CO)_5]$ (**3**) in 90% yield. An FD mass spectrum, elemental analysis and X-ray diffraction studies confirmed the composition of **3**. The IR spectrum of **3** contains absorptions at 2050, 1945, and 1895 cm^{-1} typical of the $Cr(CO)_5$ fragment, while the ν(Nb−H) frequency is too weak to be detected. The ^{1}H NMR spectrum in CD_2Cl_2 solution exhibits eight broad multiplets of equal intensity between δ = 4.64 and 6.58 at room temperature, which then sharpen at −20 °C. The observed pattern agrees with the presence of nonequivalent Cp′ rings. However, the singlet at δ = 1.31, which is characteristic for the *t*Bu groups, does not split even at low temperatures. The Nb−H resonance at δ = −2.95 is only slightly affected by coordination of the $Cr(CO)_5$ fragment compared to that of **1** (δ = −3.50). The ^2J(H-Te) coupling has disappeared. As **3** is thermally labile in solution (see below) heating of the solution in order to simplify the spectrum was not tried.

A single crystal of **3** was obtained from toluene/pentane (1:1) and studied by X-ray diffraction analysis. A bent metallocene structure with nearly eclipsed *t*Bu substituents is observed as the main structural feature (Figure 3). The Nb atom bears a Te_2 unit and an H atom both located in the plane bisecting the niobocene moiety. The Nb-coordinated hydride follows directly from the difference Fourier synthesis after refinement of all the other atoms. Thus, complex **3** is one of the few structurally characterized complexes containing a $\mu,\eta^{1:2}$-Te_2 ligand. Consequently, the structural type **B** may be assumed for precursor **1**. The Te−Te distance of 2.695(1) Å is similar to those in complexes containing side-on coordinated η^2-Te_2.[22] The coordination of the $Cr(CO)_5$ fragment at Te(2) may be responsible for two slightly different Nb−Te bonds, which are in turn in the

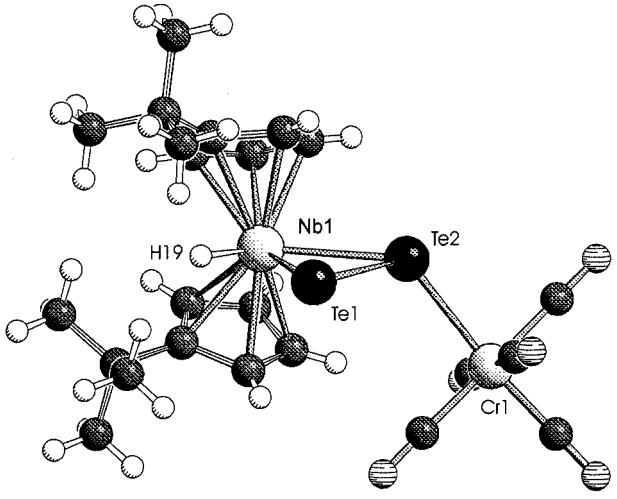

Figure 3. Molecular structure of $[Cp'_2NbTe_2H{\cdot}Cr(CO)_5]$ (**3**) (Schakal); selected distances [Å] and angles [°]: Te(1)−Te(2) 2.695(1), Te(1)−Nb(1) 2.846(1), Te(2)−Nb(1) 2.950(1), Te(2)−Cr(1) 2.712(1), Nb(1)−H(19) 1.60(5); Te(1)−Te(2)−Nb(1) 60.3(1), Te(2)−Te(1)−Nb(1) 64.3(1), Te(1)−Te(2)−Cr(1) 113.3(1), Nb(1)−Te(2)−Cr(1) 128.1(1), Te(1)−Nb(1)−H(19) 68.2(2), $C(1-5)_{center}$−Nb−$C(10-14)_{center}$ 134.1(1)

same range as Nb−Te single bonds (see complex **2**). The Te(2)−Cr distance is similar to those in other molecular chromium tellurides.[23]

The solid state structure of **2** has shown the niobocene components to be rather space filling. Therefore it was of interest to see whether the Te bridges were still sufficiently accessible for the addition of bulky Lewis acid complex fragments such as $[Cr(CO)_5]$. Indeed, reaction of THF solutions of **2** with excess $[Cr(CO)_5THF]$ gave $[Cp'_6Nb_4Te_4O{\cdot}2Cr(CO)_5]$ (**4**). Its composition follows from elemental analyses and X-ray crystallography, whereas FD mass spectra only showed the mass peak of the precursor complex **2**. The IR spectrum of **4** exhibits a CO absorption pattern typical for coordinated $Cr(CO)_5$ fragments. The ^1H NMR spectrum of **4** (Figure 2) shows six singlets for the *t*Bu groups between $\delta = 1.24$ and 1.59 and 18 multiplets for the C_5H_4 hydrogens between $\delta = 2.89$ and 6.50 at room temperature, as would be expected from the solid state structure. This result indicates that coordination of the $Cr(CO)_5$ groups gives rise to restricted rotation around the Cp′−Nb bonds in **4** at room temperature, whereas in the precursor complex **2** cooling to −90 °C is required in order to distinguish between the diastereotopic ring protons.

A crystallographic study shows **4** to possess the same structural framework as its precursor **2**. In addition, one Te bridge of each of the two four-membered Nb_2Te_2 rings bears a $Cr(CO)_5$ group (Figure 4). Upon comparing the bonding parameters of **2** and **4** (Table 1) it is evident that coordination of the $Cr(CO)_5$ fragments does not cause significant differences within the inorganic core of both molecules. Differences may only be noted for the conformations of the *t*Bu groups of the niobocene units "Nb(2)" and "Nb(4)" with respect to those of the Cp′ ligands attached at Nb(1) and Nb(3). Steric reasons may be responsible for the coordination of only two $Cr(CO)_5$ fragments at **2**. The Cr−Te−Nb angles in the range of 130° along with the acute dihedral angles (34.4°) formed by the Cr−Te bonds and the Nb_2Te_2 planes are indicative of strong steric interactions in **4** between the $Cr(CO)_5$ groups and the Cp′ ligands.

Preparation, Characterization, and Methylation of $[Cp'_4Nb_2Te_2]$ (5)

In contrast to $[Cp^*_2Nb(Te_2H)]$, which easily eliminates Te^0 units upon reaction with $[Cr(CO)_5THF]$ affording *cyclo*-$Te_4[Cr(CO)_5]_4$,[7] **1** gives the $Cr(CO)_5$ adduct **3**, whose solutions are surprisingly stable at room temperature. However, one may expect a thermal lability of **3** similar to that observed for the isostructural sulfur homologues $[Cp'_2Ta(S_2)H{\cdot}Cr(CO)_5]$[24] and $[Cp^*_2Nb(S_2)H{\cdot}Cr(CO)_5]$.[25] Solutions of these compounds readily lose CO upon heating, forming the heterotrimetallic complexes $[(Cp'_2TaS_2)_2Cr]$ and $[(Cp^*_2NbS_2)_2Cr]$, respectively.[8,9]

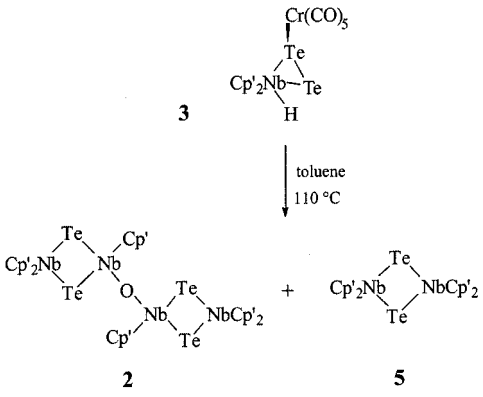

(1)

A solution of $[Cp'_2Nb(Te_2)H{\cdot}Cr(CO)_5]$ (**3**) in toluene gave green-black $[Cp'_4Nb_2Te_2]$ (**5**) upon heating, along with small amounts of **2** [Equation (1)]. Complex **5** has been obtained in still better yield from the reaction of **1** with $[Cr(CO)_6]$ in refluxing toluene.[25] The analytical and spectroscopic data of **5** are in agreement with the independently synthesized compound, the solid state structure of which has been described briefly. In this study direct bonding interactions between opposite atoms of the Nb_2Te_2 core were excluded.[25] The central feature of the structure is two niobocene units held together by two Te bridges, thus forming a planar Nb_2Te_2 core (Figure 5). As in compounds **2** and **4** the niobocene units are chiral, but the conformation found in the crystal structure of **5** corresponds to the achiral *meso* form. Although C_{2h} symmetry has been found in

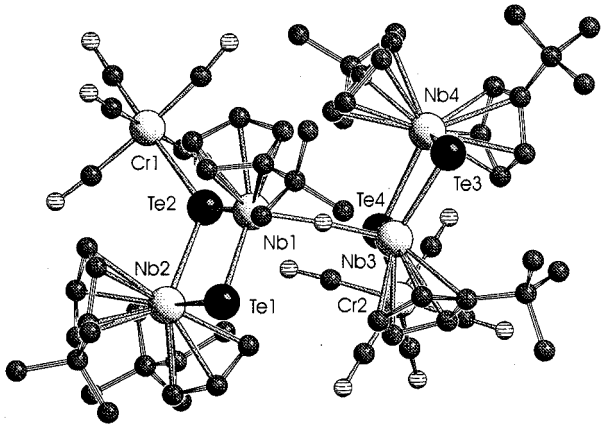

Figure 4. Molecular structure of $[Cp'_6Nb_4Te_4O{\cdot}2Cr(CO)_5]$ (**4**)

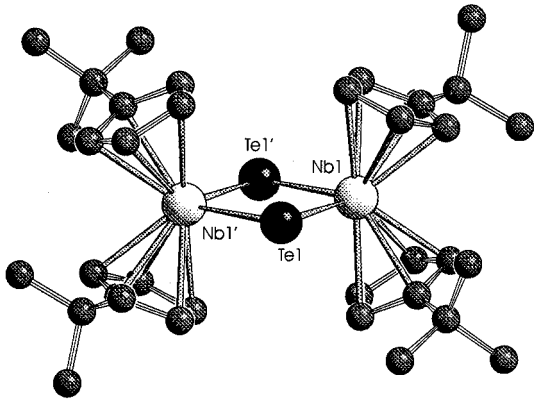

Figure 5. Molecular structure of $[Cp'_4Nb_2Te_2]$ (**5**)[25]

the related complex $[Cp'_4Zr_2Te_2]$ as well, in this complex the ^1H NMR spectra could not provide evidence for a restricted rotation around the Cp′−Zr axis.[21] In our case, examination of CD_2Cl_2 solutions reveals two signals for the C_5H_4 protons and one resonance for the *t*Bu group at ambient temperature, with splitting of the aromatic resonances into four multiplets at δ = 3.24, 4.79, 5.47, and 5.61 upon cooling to −90 °C. As expected the *t*Bu resonance remains unaffected.

Of particular interest is an analysis of the bonding system within the four-membered Nb_2Te_2 ring. In complex **5** each Nb center is surrounded by two Cp′ anions and two Te^{2-} bridges. A bonding interaction between opposite atoms Te(1) and Te(1′) [*d* = 4.262(1) Å] was excluded[25] in agreement with literature values given for planar M_2Te_2 rings: Whereas in the Ni_2Te_2 cycle of $[(iPr_4C_5H)_2Ni_2(\mu\text{-}Te)_2]$ the observed Te···Te distance of 3.052(5) Å has been ascribed to a bond order of nearly one,[26] a clearly nonbonding situation has been found in $[Cp'_4Zr_2Te_2]$ [*d*(Te···Te) = 4.006(1) Å].[21] Less evident is the interpretation of the Nb(1)···Nb(1′) distance in **5**. The found value of 3.647(1) Å is about 0.22 Å longer than that in compounds **2** and **4**. As a possibility to explain the observed diamagnetism of the molecule a through-space metal−metal coupling of both $Nb(d^1)$ centers was suggested[25] as has been recently established in the isoelectronic $[(C_5H_5)_4Zr_2(\mu\text{-}I)_2]$.[27] This direct Nb−Nb interaction has now been confirmed by DFT calculations (see below).

In order to get a better insight into the bonding system and the reactivity of **5** we decided to study methylation reactions and to carry out electrochemical studies on **5** and the reaction products. The methylation of μ_2-Te bridges in organometallic complexes has been reported recently.[28]

Green-black solutions of **5** in THF reacted with CH_3I with the formation of violet precipitates. These contain $[Cp'_4Nb_2Te(CH_3Te)]I$ ([**6**]**I**) or $[Cp'_4Nb_2(CH_3Te)_2]I_2$ ([**7**]$\mathbf{I_2}$) in quantitative yields depending on the employed stoichiometry (one or two equivalents of CH_3I). The composition of both compounds was confirmed by positive FAB mass spectra, which exhibit the peaks for the corresponding cations $[Cp'_4Nb_2Te(CH_3Te)]^+$ ([**6**]$^+$) and $[Cp'_4Nb_2(CH_3Te)_2]^{2+}$ ([**7**]$^{2+}$). The elemental analysis was close to the calculated value for [**6**]**I** and correct for [**7**]$\mathbf{I_2}$. The violet solution of [**7**]$\mathbf{I_2}$ in methanol was transformed into a dark blue precipitate in nearly quantitative yield upon addition of an aqueous solution containing two equivalents of NH_4PF_6. The composition $[Cp'_4Nb_2(CH_3Te)_2][PF_6]_2$ (**8**) roughly follows from the elemental analysis. The IR spectrum of **8** exhibits the typical absorption of the PF_6^- anion at 835 cm^{-1}. Complex **8** is poorly soluble in common solvents, thus preventing further spectroscopic investigations or recrystallization.

The ^1H NMR spectrum of [**6**]**I** (in CD_2Cl_2) shows one sharp singlet for the *t*Bu groups at δ = 1.53 and six multiplets between δ = 4.32 and 5.53 for the aromatic hydrogens. A singlet at δ = 2.45 was assigned to the μ-CH_3Te ligand. The ^1H NMR spectrum of [**7**]$\mathbf{I_2}$ (in CD_3OD) exhibits one slightly broadened singlet and two sharp singlets (intensity ratio 2:1:1) for the *t*Bu groups and eleven multiplets of different intensities between δ = 3.38 and 6.60 for the aromatic hydrogens. One sharp and one slightly broadened singlet at δ = 2.88 and 2.71, respectively, were tentatively assigned to the μ-CH_3Te ligands. From the solid state structure, which exhibits C_{2h} symmetry (see below), one might expect four equivalent Cp′ rings, i.e. one *t*Bu signal and four multiplets for the aromatic protons, provided the conformative flexibility of the Cp′ rings is blocked in solution.

The crystal structure of [**7**]$\mathbf{I_2}$ may be derived from its precursor $[Cp'_4Nb_2Te_2]$ (**5**). It contains a planar four-membered Nb_2Te_2 ring with four attached Cp′ ligands and two methyl groups, which are fixed at the Te bridges in a *trans* position (Figure 6). This arrangement, along with that of the *t*Bu groups in both niobocene units, gives rise to C_{2h} symmetry. The nonbonding Te(1)···Te(1′) distance (4.35 Å) and the angles at the Te bridges indicate that addition of electrophiles like CH_3^+ to **5** does not enhance attractive intraannular forces between the chalcogen atoms. Consequently, the positive charges may be localized at the Nb centers.

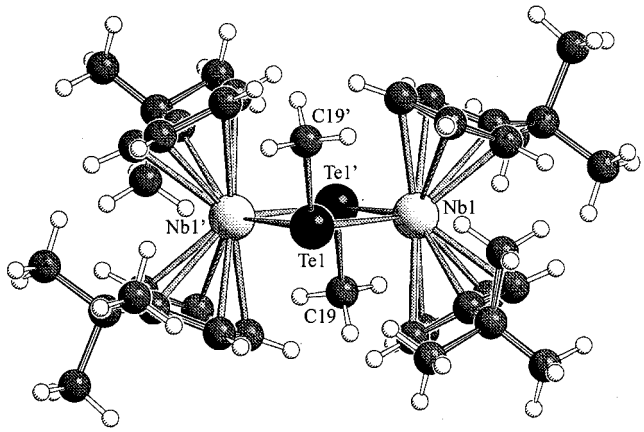

Figure 6. Molecular structure of $[Cp'_4Nb_2(CH_3Te)_2]^{2+}$ in [**7**]$\mathbf{I_2}$; selected distances [Å] and angles [°]: Nb(1)−Te(1) 2.838(3), Nb(1′)−Te(1) 2.876(4), Te(1)···Te(1′) 4.349(13), Nb(1)···Nb(1′) 3.707(9), Te(1)−C(19) 2.17(3); Nb(1)−Te(1)−Nb(1′) 80.9(1), Te(1)−Nb(1)−Te(1′) 99.1(1), Nb(1)−Te(1)−C(19′) 113.4(8), Nb(1′)−Te(1)−C(19′) 115.4(11), $C(1-5)_{center}$−Nb(1)−$C(10-14)_{center}$ 132.0(1)

The conformation found in the solid state may be caused by steric constraints, since the contacts between the $tBuC_5H_4$ hydrogens and the CH_3Te groups [*d*(H···H) ≥ 1.87 Å] are rather close. However, from the ^1H NMR spectra the presence of a further stereoisomer in solution with two nonequivalent Cp′ rings is evident. A further possibility would be an isomer with a *cis* arrangement of the CH_3Te ligands, the niobocene units being arranged as in the achiral *meso* form. Unfortunately, it was not possible to check this by dissolving separated crystals at low temperatures in order to carry out low temperature NMR investigations. However, there are some arguments supporting our hypotheses: a) Replacement of both CH_3 groups by the much bulkier $Cr(CO)_5$ groups leads to $[Cp'_4Nb_2Te_2{\cdot}2Cr(CO)_5]$ exclusively with C_{2h} symmetry. This follows from the room

temperature ^{1}H NMR spectrum, which exhibits only one singlet for the *t*Bu groups and four multiplets for the *t*BuC$_5$H$_4$ protons;[29] (b) electrochemical experiments carried out on **[7]I$_2$** (see below) confirm the homogeneity of the compound, so that a mixture of different compounds can be excluded.

Electrochemical Behavior of 5, [6]I, and [7]I$_2$

The electrochemical behavior of **5**, **[6]I**, and **[7]I$_2$** has been studied by cyclic voltammetry, rotating disk electrode (RDE) voltammetry, and electrolysis techniques. The voltammetric half-wave potentials are given in Table 2. For each compound, in the anodic area, reversible systems at +0.05 V (**5**) and +0.35 V (**[6]I**, **[7]I$_2$**) are observed, while the second oxidation steps at +0.59 V (**5**) and +0.80 V (**[6]I**, **[7]I$_2$**) are irreversible. The peaks at +0.35 and +0.80 V correspond to the oxidation of I^-.[30] The same oxidation peak potentials were obtained when Bu$_4$NI was used. In the cathodic part each complex exhibits two reversible one-electron systems in the potential range between −0.40 and −2.20 V (Figure 7). For these two reduction processes, the current ratio $i_{p,c}/i_{p,a}$ is equal to unity (or very close to it) for sweep rates v between 20 and 200 mV·s^{-1} and the peak current increases linearly with $v^{1/2}$. The half-wave potentials are independent of the potential scan rate and the peak shapes are characterized by $|E_{p,c} - E_{p,a}| \approx 60$ mV in agreement with a one-electron transfer controlled by diffusion.[31,32]

Table 2. $E_{1/2}$ values and HOMO and LUMO energies (eV) for complexes **5**, **[6]I** and **[7]I$_2$** (E values were determined with a carbon electrode vs. SCE; THF, 0.2 mol·L^{-1} Bu$_4$NPF$_6$)

	$E_{1/2\ ox2}$ [V]	$E_{1/2\ ox1}$ [V]	$E_{1/2\ red1}$ [V]	$E_{1/2\ red2}$ [V]	E_{HOMO}	E_{LUMO}
5	+0.59	+0.05	−1.83	−2.19	−4.427	−1.787
[6]I	+0.80	+0.35	−1.00	−1.34	−7.781	−5.615
[7]I$_2$	+0.80	+0.36	−0.39	−0.59	−11.414	−8.679

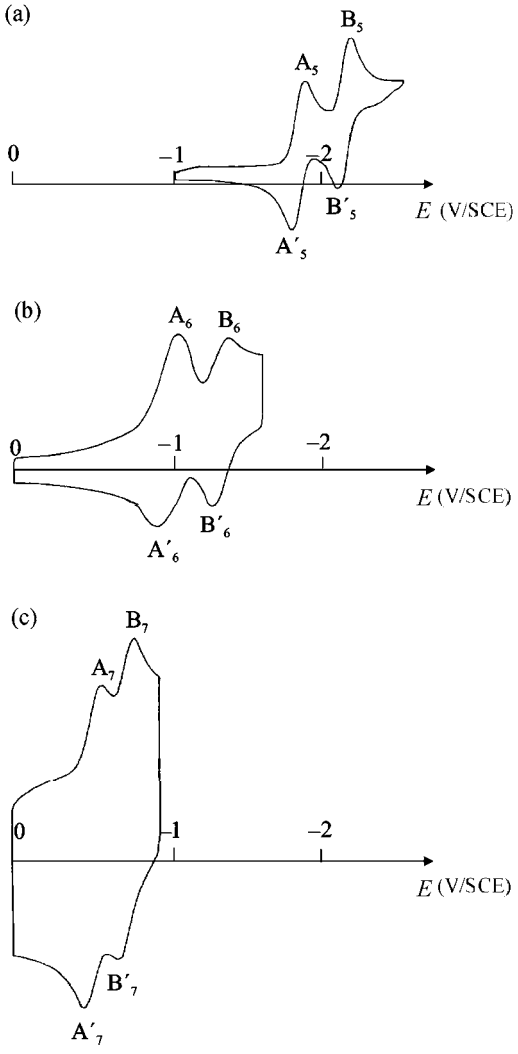

Figure 7. Cyclic voltammograms of complexes **5** (a), **[6]I** (b), and **[7]I$_2$** (c) in THF (0.2 mol·L^{-1} Bu$_4$NPF$_6$; initial potential 0 V, sweep rate 0.1 V·s^{-1})

The processes that take place during reduction of complex **5** are represented in Scheme 2a. The anionic species **[5]**$^-$ and **[5]**$^{2-}$ are relatively unstable on the electrolysis time scale and it was not possible to characterize them. In complex **[6]I**, two reversible waves are observed at −1.0 and −1.34 V, respectively. The corresponding reduction processes concern the cation **[6]**$^+$ as shown in Scheme 2b. It is interesting to note that after quantitative reduction of **[6]**$^+$ at the first reduction potential the two systems A_5/A_5' and B_5/B_5' are observed. This means that complex **5** has been reformed via quantitative CH_3 elimination. The two-electron reduction of **[6]**$^+$ leads to the very unstable monoanion **[6]**$^-$.

For complex **[7]I$_2$**, each reduction step is found by means of coulometry to correspond to a one-electron process [see (a) in Figure 8]. After reduction at −0.80 V (plateau of wave B_7), 2 F·mol^{-1} have been consumed and the color of the solution turns from opaque purple to translucent brown. The resulting species **7** (Scheme 2c) is stable even on the electrolysis time scale since no evolution of the RDE voltammogram waves (B'_7/A'_7) occurs [see (b) in Figure 8]. In order to get an ^{1}H NMR spectrum the solvent was evaporated from the electrolyzed solution and the residue extracted with toluene. Unfortunately, upon concentration the solution changed to violet. The slow evolution of **7** may also be observed in the UV spectrum.

By oxidation of solutions of **7** at −0.5 V (plateau of wave B'_7) the cation **[7]**$^+$ is obtained, which exhibits the reduction wave B_7 and the oxidation wave A'_7 [see (c) in Figure 8] as well as a ten-line ESR signal characteristic of a complex containing a paramagnetic niobium(IV) center ($a_{iso(Nb)}$ = 65 G; g_{iso} = 2.0400). The electrogenerated species **[7]**$^+$ is relatively unstable with respect to **7**, probably due to a slow partial evolution with release of CH_3, which would result in the formation of **[6]**$^+$.

We have also studied the reduction behavior of **5** in the presence of CH_3I. We have verified that **5** spontaneously

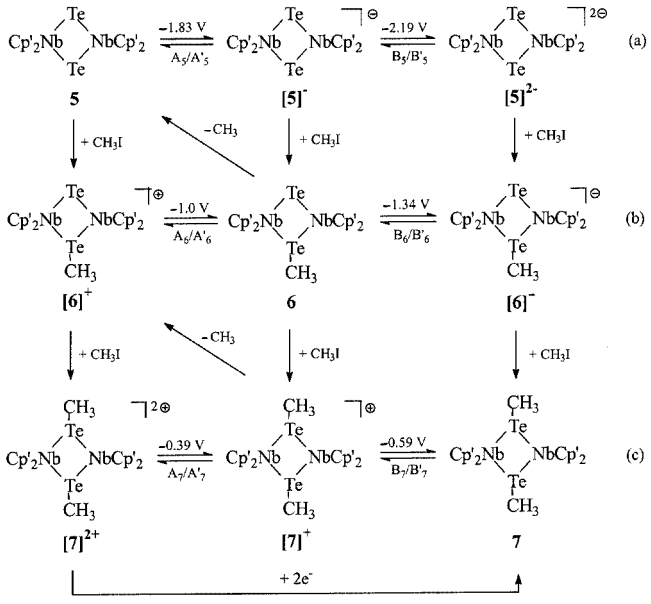

Scheme 2

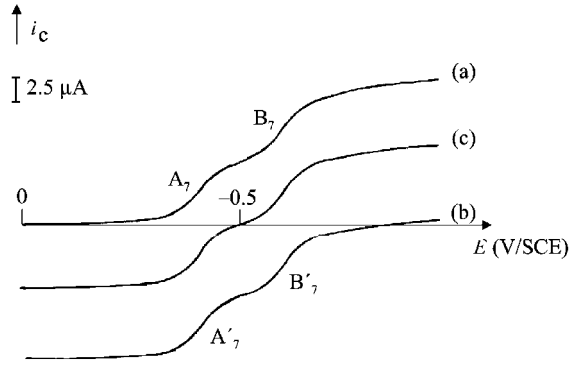

Figure 8. RDE voltammogram of [7]I_2 on carbon electrode in THF (0.2 mol·L^{-1} Bu_4NPF_6): (a) before electrolysis; (b) after 2 e^- reduction at −0.8 V; (c) after 1 e^- oxidation at −0.5 V

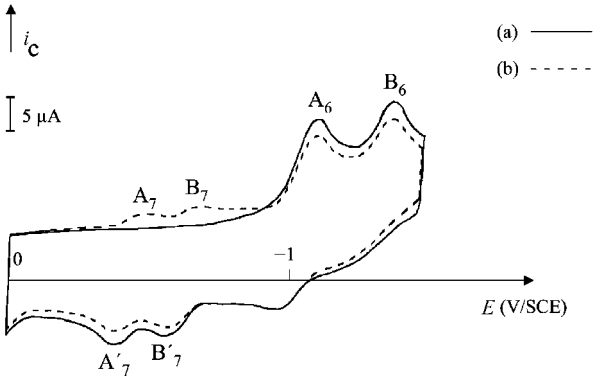

Figure 9. Cyclic voltammogram of **5** with CH_3I in THF (0.2 mol·L^{-1} Bu_4NPF_6): (a) first and (b) second sweeps. Initial potential 0 V, sweep rate 0.1 V·s^{-1}

gives $[6]^+$, for instead of the reduction peaks A_5/B_5 the peaks A_6/B_6 appear (Figure 9). When the potential sweep is reversed after B_6, two oxidation peaks A'_7 and B'_7 appear. This means that $[6]^-$ reacts quickly with CH_3I to give **7**. During the reverse sweep, peaks A_7 and B_7, characteristic of the dication $[7]^{2+}$, are observed.

The electrochemical results can be rationalized on the basis of a square scheme involving nine species. From one to the next species, one electron is exchanged horizontally (Scheme 2).

Theoretical Calculations

The bonding features of complexes **5**, $[6]^+$, and $[7]^{2+}$ have been investigated by DFT calculations. We have carried out geometry optimizations at the B3LYP/LANL2DZ level on models of these three complexes by introducing the unsubstituted C_5H_5 (Cp) ring instead of $tBuC_5H_4$ (Cp′). A full optimization yields a satisfactory agreement of calculated parameters with the experimental values for **5** and $[7]^{2+}$.[33] The most striking discrepancy has been found for the Nb−Nb distance in **5** [3.782 Å (Cp) vs. 3.647 Å (Cp′)]. The compositions and shapes of the HOMO and LUMO frontier orbitals are essentially the same for the three molecules studied. They are built of roughly a 35% contribution of 'd' atomic orbitals of each Nb atom and a 15% contribution of 'p' orbitals of each Te atom. The HOMO's exhibit a favorable Nb−Nb overlap and may be considered as metal−metal bonding orbitals while the LUMO's are the metal−metal antibonding ones. Their energies are included in Table 2. As an example, the shape of the LUMO for **5** is depicted in Figure 10.

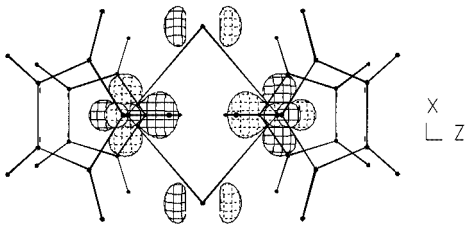

Figure 10. LUMO of **5**

The HOMO is concerned with the oxidation process, whereas the LUMO is used for reduction. As mentioned above, the oxidation waves for $[6]^+$ and $[7]^{2+}$ are probably covered by those of the I^-/I_2 system. However, the reduction potentials could be properly measured. There is a linear correlation between these reduction potentials for **5**, $[6]^+$, $[7]^{2+}$ and the calculated energies of the LUMO's of the corresponding model compounds (Table 2). Thus, the weak potential of −0.39 V is needed for reduction of $[7]^{2+}$, the LUMO of which is easily accessible for the incoming electron because of its low energy. Stronger potentials are necessary for reduction of $[6]^+$ and **5** because the energies of their LUMO's are higher. Assuming that a similar correlation (same slope) also holds for E_{HOMO} versus oxidation potential, the expected values for the first oxidation potentials should be close to 0.8 V for $[6]^+$ and 1.5 V for $[7]^{2+}$,with reference to 0.05 V, measured for **5**.

Conclusions

The reaction of $[Cp'_2NbH_3]$ with elemental tellurium gives $[Cp'_2Nb(Te_2)H]$ (**1**) in good yields. Complex **1** is a missing member of the class of group 5 dichalcogenido metallocene hydrides $[Cp_2M(X_2)H]$ (Cp = any cyclopentadienyl; M = Nb, Ta; X = S, Se, Te). In spite of some difficulties in obtaining complete analytical and spectroscopic data for **1** its structure may be deduced from the $Cr(CO)_5$ adduct **3**. Further support for the stabilization of the Nb(η^2-Te_2) moiety in the *t*Bu-niobocene part is also provided by the insertion of an $Fe_2(CO)_6$ unit into the Te−Te bond of **1**.[34] The fact that the bimetallic complex **3** gives the dinuclear, homometallic compound $[Cp'_4Nb_2Te_2]$ (**5**) under thermolytic conditions demonstrates the ability of **1** to eliminate Te. We have already shown that in the presence of suitable transition metal carbonyls **1** is a convenient Te transfer reagent for the synthesis of polymetallic metal telluride clusters.[25,35]

Experimental Section

General and Methods: All manipulations were performed with Schlenk techniques under N_2 or argon using dry solvents. Tellurium and SiO_2 (activity II-III, 63−200 μm) were degassed by several vacuum/N_2 cycles. Elemental analyses were performed at the Mikroanalytisches Laboratorium, Universität Regensburg. IR spectra were obtained with a Beckman 4240 instrument. ^{1}H NMR spectra were recorded with a Bruker ARX 400 instrument. FD and FAB mass spectra were obtained on a Finnigan MAT spectrometer. $[Cp'_2NbH_3]$ was prepared according to literature methods.[36] Electrochemistry: Cyclic voltammetry was carried out in a standard three-electrode cell with a Tacussel UAP4 unit cell. The reference electrode was a saturated calomel electrode (SCE) separated from the solution by a sintered glass disk. The auxiliary electrode was a platinum wire. For all voltammetric measurements, the working electrode was a vitreous carbon electrode. The controlled potential electrolysis was performed with an Amel 552 potentiostat coupled to an Amel 721 electronic integrator. Electrolyses were performed in a cell with three compartments separated with fritted glass of medium porosity. A carbon gauze was used as the cathode, a platinum plate as the anode and a saturated calomel electrode as the reference electrode. Computational details: All calculations on the closed shell complexes **5**, $[\mathbf{6}]^+$, and $[\mathbf{7}]^{2+}$ were performed using the GAUSSIAN 98 series of programs.[37] Density functional theory (DFT)[38] was applied with the B3LYP functional[39] and with the standard LANL2DZ basis set.[40] The input geometries for optimizations of **5** and $[\mathbf{7}]^{2+}$ were those from available X-ray data (C_5H_5 instead of $tBuC_5H_4$), while the averaged metric parameters from **5** and $[\mathbf{7}]^{2+}$ were used for the starting geometry of $[\mathbf{6}]^+$. The final wave functions and energy levels for **5**, $[\mathbf{6}]^+$, and $[\mathbf{7}]^{2+}$ were obtained from single point calculations carried out on optimized geometries at the same level of theory.

Synthesis of $[Cp'_2Nb(Te_2)H]$ (1): A mixture of $[Cp'_2NbH_3]$ (900 mg, 2.66 mmol), degassed tellurium powder (850 mg, 6.66 mmol), and freshly distilled THF (100 mL) was stirred for 48 h at 40 °C. During this time the color changed from bright brown to dark orange. After evaporation of the solvent the residue was suspended in toluene (12 mL) and transferred to the top of a chromatography column (SiO_2, column 15 × 3 cm). A dark orange band containing 1.27 g (2.15 mmol, 81%) of **1** was eluted with toluene. Red crystals were obtained from toluene/pentane (1:1). $C_{18}H_{27}NbTe_2$ (591.52): calcd. C 36.55, H 4.60; found C 35.36, H 4.25. Mol. mass 591.1 (FD-MS, toluene). ^{1}H NMR (400 MHz, CD_2Cl_2, 24 °C): δ = 6.56 (m, 2 H, C_5H_4R), 4.98 (m, 2 H, C_5H_4R), 4.74 (m, 2 H, C_5H_4R), 4.44 (m, 2 H, C_5H_4R), 1.39 (s, 18 H, CH_3), −3.50 (s, $^2J_{H,Te}$ = 86.7 Hz, 1 H, NbH). ^{125}Te{^{1}H} NMR (157 MHz, CD_2Cl_2): δ = −749.4.

Synthesis of $[Cp'_6Nb_4Te_4O]$ (2): A mixture of $[Cp'_2NbH_3]$ (900 mg, 2.66 mmol), untreated tellurium powder (850 mg, 6.66 mmol) and THF (100 mL) was stirred for 48 h at 40 °C, during which time the color changed to dark violet. After evaporation of the solvent the residue was suspended in toluene (12 mL) and chromatographed on SiO_2 (column 15 × 3 cm). A red-violet band containing $[Cp'_6Nb_4Te_4O]$ (**2**) in yields between 110 and 350 mg (0.07−0.22 mmol, 10−32%) was eluted with toluene. Then a dark orange band was eluted containing between 140 and 830 mg (0.24−1.40 mmol, 9−53%) of $[Cp'_2NbTe_2H]$ (**1**). Complex **2** was recrystallized from THF/Et_2O (4:1) $C_{54}H_{78}Nb_4OTe_4$ (1625.22): calcd. C 39.91, H 4.84; found C 40.13, H 5.01. Mol. mass 1625.7 (FD-MS, toluene). ^{1}H NMR (400 MHz, CD_2Cl_2): δ = 5.75 (m, 4 H, C_5H_4R), 5.30 (m, 4 H, C_5H_4R), 5.11 (m, 4 H, C_5H_4R), 4.88 (m, 8 H, C_5H_4R), 4.18 (m, 4 H, C_5H_4R), 1.54 (s, 18 H, CH_3), 1.47 (s, 18 H, CH_3), 1.26 (s, 18 H, CH_3).

Synthesis of $[Cp'_2Nb(Te_2)H{\cdot}Cr(CO)_5]$ (3): A solution of **1** (520 mg, 0.88 mmol) in THF (50 mL) was added to a solution of $[Cr(CO)_5THF]$ (4.40 mmol) in THF (150 mL). The mixture was stirred for 15 h at room temperature in the dark. After evaporation of the solvent the brown residue was dried under high vacuum in order to remove reformed or excess $[Cr(CO)_6]$. Then the residue was dissolved in a mixture of toluene (12 mL) and acetone (2 mL). Chromatography on SiO_2 (column 20 × 5 cm) gave a golden brown band, containing $[Cp'_2Nb(Te_2)H{\cdot}Cr(CO)_5]$ (**3**) (620 mg, 0.79 mmol, 90%), which was recrystallized from toluene/pentane (1:1). $C_{23}H_{27}CrNbO_5Te_2$ (783.56): calcd. C 35.26, H 3.47; found C 35.12, H 3.61. Mol. mass 783.7 (FD-MS, toluene). IR (KBr): $\tilde{\nu}$ = 2050 s, 1945 vs, 1895 vs cm^{-1} [ν(CO)]. ^{1}H NMR (400 MHz, CD_2Cl_2): δ = 6.58 (m, 1 H, C_5H_4R), 6.27 (m, 1 H, C_5H_4R), 5.20 (m, 1 H, C_5H_4R), 5.14 (m, 1 H, C_5H_4R), 4.87 (m, 1 H, C_5H_4R), 4.73 (m, 1 H, C_5H_4R), 4.69 (m, 1 H, C_5H_4R), 4.64 (m, 1 H, C_5H_4R), 1.31 (s, 18 H, CH_3), −2.95 (s, $^2J_{H,Te}$ = 93.0 Hz, 1 H, NbH).

Synthesis of $[Cp'_6Nb_4Te_4O{\cdot}2Cr(CO)_5]$ (4): A solution of **2** (330 mg, 0.203 mmol) in THF (50 mL) was added to a solution of $[Cr(CO)_5THF]$ (0.908 mmol) in THF (150 mL). The mixture was stirred for 15 h at room temperature in the dark. After evaporation of the solvent the residue was dissolved in toluene (15 mL). Chromatography on SiO_2 (column 15 × 3 cm) gave a broad dark red band upon elution with toluene, containing $[Cp'_6Nb_4Te_4O{\cdot}2Cr(CO)_5]$ (**4**) (310 mg, 0.154 mmol, 76%). Crystals of **4** containing 1.5 molecules of toluene were obtained from toluene. $C_{64}H_{78}Cr_2Nb_4O_{11}Te_4$ (2009.32): calcd. for **4**·1.5C_7H_8 C 41.66, H 4.22; found C 41.61, H 4.23. Mol. mass 1625.3 ($[Cp'_6Nb_4Te_4O]$ (**2**); FD-MS, toluene). IR (KBr): $\tilde{\nu}$ = 2050 s, 1975 vs, 1920 vs cm^{-1} [ν(CO)]. ^{1}H NMR (400 MHz, CD_2Cl_2): δ = 6.50 (m, 1 H, C_5H_4R), 6.42 (m, 2 H, C_5H_4R), 6.22 (m, 1 H, C_5H_4R), 5.98 (m, 1 H, C_5H_4R), 5.91 (m, 2 H, C_5H_4R), 5.85 (m, 2 H, C_5H_4R), 5.76 (m, 2 H, C_5H_4R), 5.72 (m, 1 H, C_5H_4R), 4.85 (m, 1 H, C_5H_4R), 4.70 (m, 2 H, C_5H_4R), 4.35 (m, 1 H, C_5H_4R), 4.19 (m, 1 H, C_5H_4R), 4.05 (m, 1 H, C_5H_4R), 3.87 (m, 1 H, C_5H_4R), 3.83 (m, 1 H, C_5H_4R), 3.51 (m, 1 H, C_5H_4R), 3.20 (m, 1 H, C_5H_4R), 2.89 (m, 2 H,

C_5H_4R), 1.59 (s, 9 H, CH_3), 1.55 (s, 9 H, CH_3), 1.45 (s, 9 H, CH_3), 1.40 (s, 9 H, CH_3), 1.28 (s, 9 H, CH_3), 1.24 (s, 9 H, CH_3).

Thermolysis of $[Cp'_2NbTe_2H{\cdot}Cr(CO)_5]$ (3): A solution of **3** (350 mg, 0.447 mmol) in toluene (120 mL) was stirred for 15 h at 110 °C in the dark. Then the solvent was removed in vacuo and the residue was purified by chromatography on SiO_2 (column 15 × 3 cm). Elution with toluene first gave a red-violet band containing $[Cp'_6Nb_4Te_4O]$ (**2**) (25 mg, 0.015 mmol, 14%) and then a black-green band was eluted containing $[Cp'_4Nb_2Te_2]$ (**5**) (130 mg, 0.140 mmol, 63%). $C_{36}H_{52}Nb_2Te_2$ (925.81): calcd. C 46.70, H 5.66; found C 45.78, H 5.69. Mol. mass 925.6 (FD-MS, toluene). ^{1}H NMR (400 MHz, CD_2Cl_2, 24 °C): δ = 5.05 (m, 8 H, C_5H_4R), 4.46 (m, 8 H, C_5H_4R), 1.44 (s, 36 H, *t*Bu).

Synthesis of $[Cp'_4Nb_2Te(CH_3Te)]I$ ([6]I): A black-green solution of **5** (130 mg, 0.140 mmol) in THF (50 mL) was treated with CH_3I (19.9 mg, 0.140 mmol). While stirring the mixture at room temperature it turned slightly violet and a fine precipitate formed. After 30 min the solvent was evaporated in vacuo and the residue was washed twice with pentane. The resulting powder was dried under high vacuum to give **[6]I** in quantitative yield. **[6]I** was recrystallized from CH_2Cl_2/pentane (3:1). **[6]I:** $C_{37}H_{55}INb_2Te_2$ (1067.75): calcd. C 41.62, H 5.19; found C 41.58, H 4.67. Mol. mass 941.1 $\{[Cp'_4Nb_2Te(TeCH_3)]^+$ ($[\mathbf{6}]^+$); PI-LSIMS, NBA/MeOH$\}$. ^{1}H NMR (400 MHz, CD_2Cl_2, 24 °C): δ = 5.53 (m, 4 H, C_5H_4R), 5.21 (m, 2 H, C_5H_4R), 5.01 (m, 2 H, C_5H_4R), 4.67 (m, 2 H, C_5H_4R), 4.62 (m, 2 H, C_5H_4R), 4.32 (m, 4 H, C_5H_4R), 1.53 (s, 36 H, CH_3), 2.45 (s, 3 H, $TeCH_3$). UV/Vis **[6]I**: λ_{max} = 553 nm (ε = 3460 $L{\cdot}mol^{-1}{\cdot}cm^{-1}$ in CH_3OH).

Synthesis of $[Cp'_4Nb_2(CH_3Te)_2]I_2$ ([7]I_2): The procedure is analogous to that described for the synthesis of **[6]I** with the exception that two equivalents of CH_3I were employed. Recrystallization of $[Cp'_4Nb_2(CH_3Te)_2]I_2$ ([7]I_2) from CH_3OH gave violet needles. $C_{38}H_{58}I_2Nb_2Te_2$ (1209.65): calcd. C 37.72, H 5.03; found C 37.50, H 5.08. Mol. mass 956.3 $\{[Cp'_4Nb_2(CH_3Te)_2]^+$ ($[\mathbf{7}]^+$); PI-LSIMS, NBA/MeOH$\}$. ^{1}H NMR (400 MHz, CD_3OD, 24 °C): δ = 6.61 (m, 1 H, C_5H_4R), 6.55 (m, 2 H, C_5H_4R), 6.43 (m, 1 H, C_5H_4R), 5.89 (m, 1 H, C_5H_4R), 5.62 (m, 2 H, C_5H_4R), 5.53 (m, 1 H, C_5H_4R), 5.10 (m, 2 H, C_5H_4R), 4.60 (m, 2 H, C_5H_4R), 4.21 (m, 1 H, C_5H_4R), 4.11 (m, 2 H, C_5H_4R), 3.38 (m, 1 H, C_5H_4R), 2.88 (s, 3 H, $TeCH_3$), 2.71 (s, 3 H, $TeCH_3$), 1.53 (s, 18 H, CH_3), 1.51 (s, 9 H, CH_3), 1.50 (s, 9 H, CH_3). UV/Vis [7]I_2: λ_{max} = 550 nm (ε = 9120 $L{\cdot}mol^{-1}{\cdot}cm^{-1}$ in CH_3OH).

Synthesis of $[Cp'_4Nb_2(CH_3Te)_2][PF_6]_2$ (8): A solution of NH_4PF_6 (22 mg, 0.135 mmol) in H_2O (3 mL) was added to a solution of [7]I_2 (80 mg, 0.07 mmol) in MeOH (10 mL). While stirring the violet mixture for 30 min at room temperature a dark blue precipitate formed. This precipitate was separated by filtration and washed three times with small amounts of H_2O and Et_2O. The crude product was dissolved in hot acetonitrile (20 mL) and filtered. Evaporation of the solvent and drying under high vacuum gave $[Cp'_4Nb_2(CH_3Te)_2][PF_6]_2$ (**8**) (75 mg, 0.060 mmol, 91%). $C_{38}H_{58}F_{12}Nb_2P_2Te_2$ (1245.80): calcd. C 36.63, H 4.69; found C 37.72, H 4.80. IR (KBr): $\tilde{\nu}$ = 835 vs cm^{-1} [$\nu(PF_6)$].

X-ray Structure Determination: The structures of **2**, **3**, **4**, and [7]I_2 were solved by direct methods (Table 3). Subsequent difference Fourier syntheses revealed the position of the non-hydrogen atoms

Table 3. Summary of crystallographic data

	2	**3**	**4·1.5C_7H_8**	**[7]$I_2{\cdot}CH_3OH$**
Formula	$C_{54}H_{78}Nb_4OTe_4$	$C_{23}H_{27}CrNbO_5Te_2$	$C_{74.5}H_{90}Cr_2Nb_4O_{11}Te_4$	$C_{39}H_{62}I_2Nb_2OTe_2$
MW	1625.22	783.56	2147.52	1241.69
Cryst syst	Triclinic	Monoclinic	Monoclinic	Triclinic
Space group	$P\bar{1}$	$P2_1/a$	$P2_1/n$	$P\bar{1}$
a [Å]	12.0353(11)	14.9510(8)	18.6414(9)	10.512(4)
b [Å]	15.4884(15)	10.1946(8)	20.3497(10)	10.803(5)
c [Å]	17.1097(15)	17.3753(10)	21.6608(10)	11.348(4)
α [deg]	82.831(11)	90	90	72.260(4)
β [deg]	84.058(11)	98.006(7)	103.986(6)	69.100(4)
γ [deg]	68.136(10)	90	90	87.740(5)
V [Å^3]	2931.2(5)	2622.5(3)	7973.4	1143.2
Z	2	4	4	1
$d_{calcd.}$ [g/cm^3]	1.841	1.985	1.793	1.804
F(000)	1564	1496	4188	596
Cryst size [mm^3]	0.40 × 0.10 × 0.09	0.40 × 0.28 × 0.11	0.38 × 0.27 × 0.19	0.16 × 0.06 × 0.03
Diffractometer	STOE-IPDS	STOE-IPDS	STOE-IPDS	STOE-IPDS
Temp [K]	297	173	173	297
θ [deg]	2.08−25.96	2.32−25.83	1.64−25.83	2.73−26.33
No. of reflns collected	26993	29053	46068	16022
No. of indep reflns	10649	4995	14273	4117
R_{int}	0.0180	0.0387	0.0720	0.1970
No. obsd. reflections [$I > 2\sigma(I)$]	8388	4618	8396	1557
μ [mm^{-1}]	2.75	3.06	2.31	3.13
No. of data/restraints/params	10649/0/568	4995/0/325	14273/0/805	4177/0/200
GOF on F^2	0.877	1.115	0.785	0.946
Absorption correction	numerical	numerical	numerical	none
T_{max}, T_{min}	0.8216, 0.6197	0.7403, 0.3852	0.9581, 0.8758	
*R*1, *wR*2 [$I > 2\sigma(I)$]	0.0228, 0.0584	0.0267, 0.0713	0.0361, 0.0640	0.1269, 0.3169
*R*1, *wR*2 (all data)	0.0311, 0.0633	0.0292, 0.0723	0.0818, 0.0714	0.2105, 0.3660

and all these atoms were refined with anisotropic thermal parameters with the exception of **[7]I_2**. Hydrogen atoms were introduced on idealized positions and refined using a riding model. The H atom H(19) fixed at the Nb atom in the structure of **3** was formed in the difference Fourier synthesis as the third peak (0.7 electrons). After refinement the *R* values decreased significantly. The residual electron density of 2.868 e·Å^{-3} that was found after all refinement cycles is in the proximity (0.91 Å) of Te(1). The structure solution of **[7]I_2** was handicapped by a poor crystal quality. In this case refinement with anisotropic temperature factors was only possible for the heavy atoms. A void at *x*, *y*, *z* = 0, 0.5, 0.5 was localized with the program SQUEEZE.[41] It has a volume of 161 Å^3 and contains 11 electrons. This roughly corresponds to one molecule of methanol.

Crystallographic data (excluding structure factors) for the structures reported in this paper have been deposited with the Cambridge Crystallographic Data Centre as supplementary publication nos. CCDC-172951 (**2**), CCDC-172952 (**3**), CCDC-172953 (**4**), and CCDC-172954 (**[7]I_2**). These data can be obtained free of charge at www.ccdc.cam.ac.uk/conts/retrieving.html [or from the Cambridge Crystallographic Data Centre, 12, Union Road, Cambridge CB2 1EZ, UK; Fax: (internat.) +44−1223/336-033; E-mail: deposit@ccdc.cam.ac.uk].

Acknowledgments

We thank Prof. Dr. B. Wrackmeyer for recording the ^{125}Te NMR spectrum of **1**. We are grateful to the Deutsche Forschungsgemeinschaft for support of this work (Wa 485/6-2). Parts of this work were supported by the Deutscher Akademischer Auslandsdienst and the jyMinistère des Affaires Etrangères (program PROCOPE).

[1] J. M. Fischer, W. E. Piers, L. R. MacGillivray, M. J. Zaworotko, *Inorg. Chem.* **1994**, *34*, 2499−2500.
[2] [2a] G. Tainturier, M. Fahim, B. Gautheron, *J. Organomet. Chem.* **1989**, *373*, 193−202. [2b] G. Tainturier, M. Fahim, G. Trouvé-Bellan, B. Gautheron, *J. Organomet. Chem.* **1989**, *376*, 321−332.
[3] [3a] W. A. Howard, G. Parkin, A. L. Rheingold, *Polyhedron* **1994**, *14*, 25−44. [3b] J. H. Shin, T. Hascall, G. Parkin, *Organometallics* **1999**, *18*, 6−9.
[4] J. H. Shin, G. Parkin, *Organometallics* **1995**, *13*, 2147−2149.
[5] J. H. Shin, G. Parkin, *Organometallics* **1994**, *14*, 1104−1106.
[6] H. Brunner, M. Kubicki, J.-C. Leblanc, W. Meier, C. Moise, A. Sadorge, B. Stubenhofer, J. Wachter, R. Wanninger, *Eur. J. Inorg. Chem.* **1999**, 843−848.
[7] O. Blacque, H. Brunner, M. M. Kubicki, B. Nuber, B. Stubenhofer, J. Wachter, B. Wrackmeyer, *Angew. Chem. Int. Ed. Engl.* **1997**, *36*, 352−353.
[8] H. Brunner, G. Gehart, M. M. Kubicki, E. Lehrl, D. Lucas, W. Meier, Y. Mugnier, B. Nuber, B. Stubenhofer, J. Wachter, *J. Organomet. Chem.* **1996**, *510*, 291−295.
[9] O. Blacque, H. Brunner, M. M. Kubicki, D. Lucas, W. Meier, Y. Mugnier, B. Nuber, B. Stubenhofer, J. Wachter, *J. Organomet. Chem.* **1998**, *564*, 71−79.
[10] H. Brunner, D. Lucas, T. Monzon, Y. Mugnier, B. Nuber, B. Stubenhofer, A. C. Stückl, J. Wachter, R. Wanninger, M. Zabel, *Chem. Eur. J.* **2000**, *6*, 493−503.
[11] H. Brunner, J. Wachter, R. Wanninger, M. Zabel, *J. Organomet. Chem.* **2000**, *603*, 135−137.
[12] [12a] H. Brunner, G. Gehart, W. Meier, B. Nuber, J. Wachter, *J. Organomet. Chem.* **1993**, *454*, 117−122. [12b] J.-C. Leblanc, C. Moise, F. Volpato, H. Brunner, G. Gehart, J. Wachter, B. Nuber, *J. Organomet. Chem.* **1995**, *485*, 237−242.
[13] H.-J. Bach, H. Brunner, J. Wachter, M. M. Kubicki, J.-C. Leblanc, C. Moise, F. Volpato, B. Nuber, M. L. Ziegler, *Organometallics* **1992**, *11*, 1403−1407.
[14] An analysis of the linear M−O−M bridging moiety is given in: J. W. Faller, Y. Ma, *J. Organomet. Chem.* **1988**, *340*, 59−69.
[15] H. Brunner, J.-C. Leblanc, D. Lucas, W. Meier, C. Moise, Y. Mugnier, B. Nuber, S. Rigny, A. Sadorge, J. Wachter, *J. Organomet. Chem.* **1998**, *566*, 203−210.
[16] [16a] W. Tremel, *J. Chem. Soc., Chem. Commun.* **1992**, 126−128. [16b] H. Kleinke, W. Tremel, *Chem. Commun.* **1999**, 1175−1176.
[17] O. M. Kekia, A. L. Rheingold, *J. Organomet. Chem.* **1997**, *545*, 277−280.
[18] J. Emsley, *The Elements*, Clarendon Press, Oxford **1989**, 186.
[19] Yu. V. Skripkin, I. L. Eremenko, A. A. Pasynskii, Yu. T. Struchkov, V. E. Shklover, *J. Organomet. Chem.* **1985**, *267*, 285−292.
[20] L. G. Guggenberger, *Inorg. Chem.* **1973**, *12*, 294−301.
[21] G. Erker, R. Nolte, G. Tainturier, A. Rheingold, *Organometallics* **1989**, *8*, 454−460.
[22] Te−Te bonds in other monomeric η^2-Te$_2$ complexes: [22a] [Cp*$_2$Ti(Te$_2$)] [2.703(2) Å].[1] [22b] [Cp*$_2$Zr(Te$_2$)CO] [2.688(1) Å].[3] [22c] [W(PMe$_3$)(CN*t*Bu)$_4$(Te$_2$)] [2.680(2) Å]: D. Rabinovich, G. Parkin, *J. Am. Chem. Soc.* **1993**, *115*, 9822−9823. [22d] [triphosNi(Te$_2$)] [2.668(1) Å]: M. Di Vaira, M. Peruzzini, P. Stoppioni, *Angew. Chem. Int. Ed. Engl.* **1987**, *26*, 916−918.
[23] [23a] W. A. Flomer, S. C. O′ Neal, J. W. Kolis, D. Jeter, A. W. Cordes, *Inorg. Chem.* **1988**, *27*, 969−971. [23b] L. C. Roof, W. T. Pennington, J. W. Kolis, *Inorg. Chem.* **1992**, *31*, 2056−2064. [23c] S. Stauf, C. Reisner, W. Tremel, *Chem. Commun.* **1996**, 1749−1750.
[24] H. Brunner, G. Gehart, J.-C. Leblanc, C. Moise, B. Nuber, B. Stubenhofer, F. Volpato, J. Wachter, *J. Organomet. Chem.* **1996**, *517*, 47−51.
[25] H. Brunner, J. Wachter, R. Wanninger, M. Zabel, *Eur. J. Inorg. Chem.* **2001**, 1151−1154.
[26] H. Sitzmann, D. Saurenz, G. Wolmershäuser, A. Klein, R. Boese, *Organometallics* **2001**, *20*, 700−705.
[27] [27a] M. M. Rohmer, M. Bénard, *Organometallics* **1991**, *10*, 157−163. [27b] R. L. DeKock, M. A. Peterson, L. E. L. Reynolds, L.-H. Chen, E. J. Baerends, P. Vernooijs, *Organometallics* **1993**, *12*, 2794−2805.
[28] W. A. Herrmann, J. Rohrmann, C. Hecht, *J. Organomet. Chem.* **1985**, *290*, 53−61.
[29] R. Wanninger, PhD thesis, Universität Regensburg **2000**.
[30] E. Samuel, D. Guery, J. Vedel, *J. Organomet. Chem.* **1984**, *263*, C43.
[31] R. W. Murray, C. N. Reitley, *Electroanalytical principles*, Interscience, New-York, **1963**.
[32] R. S. Nicholson, *Anal. Chem.* **1965**, *35*, 1351.
[33] Calculated parameters are given in the order **5**, [**6**]$^+$, [**7**]$^{2+}$: *d*(Nb−Nb): 3.7817, 3.6625, 3.6863 Å; *d*(Te−Te): 4.228, 4.377, 4.493 Å; *d*(Nb−Te): 2.834, 2.823(Te) and 2.884(TeMe), 2.890 Å.
[34] M. Brandl, H. Brunner, J. Wachter, M. Zabel, *Organometallics*, accepted.
[35] H. Brunner, A. C. Stückl, J. Wachter, R. Wanninger, M. Zabel, *Angew. Chem. Int. Ed.* **2001**, *40*, 2463−2465.
[36] J. A. Labinger, *Adv. Chem. Ser.* **1978**, *167*, 149.
[37] M. J. Frisch, G. W. Trucs, H. B. Schlegel, G. E. Scuseria, M. A. Robb, J. R. Cheeseman, V. G. Zakrzewski, J. A. Montgomery, R. E. Stratman, J. C. Burant, S. Dapprich, J. M. Millam, A. D. Daniels, K. N. Kudin, M. C. Strain, O. Farkas, J. Tomasi, V. Barone, M. Cossi, R. Cammi, B. Mennucci, C. Pomelli, C. Adamo, S. Clifford, J. Ochterski, G. A. Petersson, P. Y. Ayala, Q. Cui, K. Morokuma, D. K. Malick, A. D. Rabuck, K. Raghavachari, J. B. Foresman, J. Cioslowski, J. V. Ortiz, B. B. Stefanov, G. Liu, A. Liashenko, P. Piskorz, I. Komaromi, R. Gomperts, R. T. Martin, D. J. Fox, T. Keith, M. A. Al-Laham,

C. Y. Peng, A. Nanayakkara, C. Gonzalez, M. Challacombe, P. M. W. Gill, B. G. Johnson, W. Chen, M. W. Wong, J. L. Andres, M. Head-Gordon, E. S. Replogle, J. A. Pople, *GAUSSIAN98* (Rev. A.6), Gaussian, Inc., Pittsburgh PA, **1998**.
[38] R. G. Parr, W. Yang, *Density Functional Theory of Atoms and Molecules*, Oxford University Press, Oxford, UK, 1989.
[39] A. D. Becke, *J. Chem. Phys.* **1993**, *98*, 5648.
[40] T. H. Dunning, Jr., P. J. Hay, in *Modern Theoretical Chemistry* (Ed.: H. F. Schaefer, III), Plenum Press, New York, **1976**, p. 1; P. J. Hay, W. R. Wadt, *J. Chem. Phys.* **1985**, *82*, 270; P. J. Hay, W. R. Wadt, *J. Chem. Phys.* **1985**, *82*, 284; P. J. Hay, W. R. Wadt, *J. Chem. Phys.* **1985**, *82*, 299.
[41] P. v. d. Sluis, A. L. Spek, *Acta Crystallogr., Sect. A* **1990**, *46*, 194.

Received October 30, 2001
[I01423]